Send Orders for Reprints to reprints@benthamscience.net

Anti-Cancer Agents in Medicinal Chemistry, **XXXX,** *XX,* **1-9**

RESEARCH ARTICLE

In-silico Evaluation of Novel Honokiol Derivatives against Breast Cancer Target Protein LKB1

Izzah Shahid[1,*], Muhammad Shoaib[2], Rabail Zehra Raza[3], Muhammad Jahangir[4], Sumra Wajid Abbasi[3], Areej Riasat[5], Ansa Akbar[1] and Samina Mehnaz[6]

[1]Department of Biotechnology, Faculty of Science and Technology, University of Central Punjab, Lahore, Pakistan; [2]Nishtar Medical College Multan, University of Health Sciences, Lahore, Pakistan; [3]NUMS Department of Biological Sciences, Faculty of Multidisciplinary Studies, National University of Medical Sciences, Rawalpindi, Pakistan; [4]Food and Biotechnology Research Center, Pakistan Council of Scientific and Industrial Research, PCSIR Laboratories Complex, Lahore, Pakistan; [5]Department of Biochemistry, Government College University Faisalabad, Faisalabad, Pakistan; [6]Kauser Abdulla Malik School of Life Sciences, Forman Christian College (A Chartered University), Lahore, 54600, Pakistan

Abstract: ***Background*:** Breast cancer is characterized by uncontrolled cell growth in the breast tissue and is a leading cause of death globally. Cytotoxic effects and reduced efficacy of currently used therapeutics insist to look for new chemo-preventive strategies against breast cancer. LKB1 gene has recently been categorized as a tumor suppressor gene where its inactivation can cause sporadic carcinomas in various tissues. Mutations in the highly conserved LKB1 catalytic domain lead to the loss of function and subsequently elevated expression of pluripotency factors in breast cancer.

***Objective*:** The utilization of drug-likeness filters and molecular simulation has helped evaluate the pharmacological activity and binding abilities of selected drug candidates to the target proteins in many cancer studies.

***Methods*:** The current *in silico* study provides a pharmacoinformatic approach to decipher the potential of novel honokiol derivatives as therapeutic agents against breast cancer. AutoDock Vina was used for molecular docking of the molecules. A 100 nano second (ns) molecular dynamics simulation of the lowest energy posture of 3'-formylhonokiol-LKB1, resulting from docking studies, was carried out using the AMBER 18.

***Results*:** Among the three honokiol derivatives, ligand-protein binding energy of 3' formylhonokiol with LKB1 protein was found to be the highest *via* molecular docking. Moreover, the stability and compactness inferred for 3'-formylhonokiol with LKB1 are suggestive of 3' formylhonokiol being an effective activator of LKB1 *via* simulation studies.

***Conclusion*:** It was further established that 3'- formylhonokiol displays an excellent profile of distribution, metabolism, and absorption, indicating it is an anticipated future drug candidate.

ARTICLE HISTORY

Received: August 11, 2022
Revised: December 18, 2022
Accepted: December 29, 2022

DOI:
10.2174/1871520623666230330083630

Keywords: Honokiol, breast cancer, molecular docking, virtual screening, LKB1, ADMET analysis.

1. INTRODUCTION

Despite the significant advances in cancer remedial methods and therapeutics, breast cancer is one of the leading causes of mortality among women. Despite the continuous development of focused screening programs and the development of targeted medication procedures, increasing breast-cancer-related mortalities are still alarming. Low efficacy, therapeutic resistance, and morbidity confine the rate of success of existing procedures. Hence, the development of effective and more potent anti-cancerous agents is an extensively researched area because of the unique pathophysiology of tumors and the evolution of resistance to therapeutics [1]. Subsequently, due to the limitations of the classical cancer remedial methods including immunotherapy, chemotherapy, and radiotherapy, research is focused on determining less toxic phytochemicals with pharmacological and bioactive potential [2].

*Address correspondence to this author at the Department of Biotechnology, Faculty of Science and Technology, University of Central Punjab, Lahore, Pakistan; Tel: +92-4235880007; Fax: +92-42-35954892;
E-mail: izzah.shahid@ucp.edu.pk

Constitutive bioactive components in the stem, leaves, roots, and bark of plants have been extensively used in traditional medicine and still are in practice. Among such plants, *Magnolia* spp. was used for centuries for the treatment of gastrointestinal disorders, stroke, dizziness, and nervousness. The complete biochemical profiles of these plants have shown the production of biologically active phenolics, flavonoids, and others. Honokiol (3',5-di-(2-propenyl)-1,1'-biphenyl-2,4'-diol) is a phenolic phytochemical derived from the seed cones of *Magnolia grandiflora* and has been extensively evaluated for antioxidant, antibacterial, antithrombolytic, and anti-inflammatory potential [3].

Moreover, the anticancer properties of honokiol have also been demonstrated *in vitro* and preclinical models, particularly in breast cancer [4]. Insights into the molecular mechanisms of honokiol demonstrate inhibition of tumor invasion and metastasis by suppression of NF-kB, PI3K/AKT/mTOR, and Ras/ERK pathways [5, 6]. Autosomal dominant mutations in the genes including BARCA1, BARCA2, LKB1, and CHEK lead to tumor progression. Among these genes, Liver Kinase B1 (LKB1) is an upstream kinase that modulates several cellular functions including tumor suppres-

sion and apoptosis. LKB1 also regulates several downstream signaling pathways through phosphorylation of 14 AMP-dependent protein kinase (AMPK)-related kinases, which lead to suppression of mTOR [7]. Mutations in the highly conserved LKB1 catalytic domain lead to the loss of function, acquiring elevated expression of pluripotency factors [8]. Similarly, honokiol has been shown to lead to apoptosis through the activation of the caspase cascade in chronic lymphocytic leukemia [9]. Interference of honokiol in the NF-κB signaling pathway results in reduced expression of downstream genes in embryonic kidney cells, promyelocytic leukemia, multiple myeloma, cervical cancer, and specifically breast cancer. Several research studies targeting the antitumor effects of honokiol alone and in combination with other anti-cancerous agents have been explored against breast cancer. However, there are hardly any reports which evaluate the three-dimensional structures and the pharmaceutical potential of honokiol derivatives through *in silico* studies. Molecular docking studies of honokiol derivatives were carried out to know their interaction with LKB1 protein. The docking results were further strengthened by molecular dynamic simulation studies and derivatives were analyzed for blood-brain barrier and gastrointestinal absorption.

2. MATERIALS AND METHODS

2.1. Gene Sequence and Mutation Analysis

The sequence of LKB1 gene was accessed from NCBI with accession number U63333. The retrieved sequence was analyzed for mutations following the verification of detected mutations through different computational platforms. Mutations were analyzed using polymorphism phenotypic-2 (Polyphene-2), which predicted the possible impact of an amino acid substitution on the structure and function of the selected LKB1 protein. The functional analysis and annotations were based on the output scores and were performed by mapping the query sequence (nsSNP) to the transcript of genes following the extraction of structure and protein sequences [10]. The detrimental effects of amino acid substitution on protein function were assessed using SIFT by homology sequencing. The output score predicted and classified the amino acid substitution as tolerant and intolerant [11]. Prediction of human deleterious single nucleotide polymorphism (PHD-SNP) was used to classify nsSNP as disease-related or neutral ones. The tool work on the basis of SVM and provide information on a new residue at a specific position [12]. MutPred2 was used to analyze impactful missense variants of disease-related and neutral amino acids. The G-value of the input sequence showed confident hypotheses, very confident hypotheses, and actionable hypotheses for their effects on protein sequences [13]. I-Mutant 2.0 was used to assess the automatic prediction of the stability changes in a protein following a single-point mutation. The results were noted as the free energy changes denoted by ΔΔG value and were based upon protein structure and sequence [14]. PROVEAN (Protein Variation Effect Analyzer) was used to perform random forest-based binary classification determining the relationship of the output score with disease and the biological function of the protein [15].

2.2. Secondary Structure Prediction

Secondary structure prediction was made using PSIPRID [16]. It helped in the prediction of the position of helix and beta-strands in a protein structure to determine the nature of the protein.

2.3. Homology Modelling of 3D Structure of Protein

Iterative Threading Assembly Refinement (I- TASSER) was used to generate the high-quality 3D structure of the protein [17]. Selection of the structure was based upon a confidence score (C-Value), where and higher C-Value indicated the consistency of the model. The alignment based upon TM-score and RSMD between query and known structures was searched in PDB (Protein Data Bank) library.

2.4. Ligand Identification and Retrieval

Three honokiol derivatives indicating anti-inflammatory and anti-cancerous activities were identified from the literature to be used as potential ligands. The 3D structures of each derivative were downloaded from PubChem [18].

2.5. Molecular Docking

Molecular docking was performed to determine the binding sites between the target molecule and ligand to form a complex. AutoDock Vina was used for molecular docking of the molecules. Protein 3D structure was retrieved from I-TASSER in PDB format. Following the addition of polar hydrogen in the protein, it was initialized as a macromolecule by using the MGL tool [19]. The active site was identified by the Computed Atlas of Surface Topography of Protein (CASTp 3.0), which predicted the amino acids on the target molecule for the potential ligand binding [20]. The grids were adjusted on the active site of the target by setting x, y, and z centers and sizes. Ligand preparation of retrieved sequences was performed following the addition of a torsional angle in the ligands.

Output files after processing from AutoDock Vina were chosen on the basis of high-affinity values and visualized on PyMol [21]. Ligand binding positions of amino acids were determined in addition to the analysis of polar, hydrophobic and pi interactions between ligand and target molecule. Molecular docking was accomplished with the PatchDock platform and results were acquired based on complementary shape criteria [22]. The algorithm consisted of three main stages including representation of the shape of the molecule, matching of surfaces patches, filtering, and scoring. Protein-ligand interaction profiler (PLIP), was used for the prediction of non-covalent bonds between the ligand and target molecule and determined the interaction between honokiol derivatives and LKB1 protein [23].

2.6. Molecular Dynamic Simulation

Docking results were further validated using molecular dynamic simulation analysis. Simulation analysis was performed to predict the binding of honokiol derivatives to LKB1 protein and to analyze the changes in binding strength with a change in the temperature. The simulation analysis was also performed to study the physical movements of the atoms of the receptor in the presence and absence of the compound for a known time. A 100 nanosecond (ns) molecular dynamics (MD) simulation of the lowest energy posture of 3' formylhonokiol-LKB1, resulting from docking studies, was carried out using the AMBER 18 software [24]. Optimization of the three-dimensional structure of the protein was performed using Gaussian 09 on applying B3LYP/6-31G (d) basis [25]. Related parameters of the screened compounds were performed using an antechamber module of AMBER suite molecular dynamics software utilizing Generalized Amber Force Field (GAFF). The input files were used to run by xleap command using Amber ff14SB force field for the created parameter and coordinate files [26, 27]. The topology files of protein and ligand were recorded using the Leap module [28]. The system was first solvated with water molecules (TIP3PBOX) followed by neutralization with sodium (Na^+) ions. Solvate box TIP3P 10.0 was added with a 10 Å buffering distance [29]. Initial velocities were based on Maxwell-Boltzmann distribution with a temperature of 300 K and constant volume (ntb = 1) for 20 ps (nstlim = 10000 × dt = 0.002) simulation time during the process of thermalization. The neutralized system was then put through a pre-processing stage that included minimization, heating, and equilibration. Berendsen thermostat was used to equilibrate the receptor or its complex at 300 K and 1 bar for constant pressure (ntp = 1) for another 500 ps simulation time. The Ewald summation method was

used to complete the MD simulation run [30]. The trajectories were analyzed using QtGrace (https://sourceforge.net/projects/qtgrace/files/). iMODS analysis was used to stimulate molecular dynamics to aid in the exploration of normal mode analysis (NMA) and to generate accessible information about routes which may include homologous structures or macromolecules. iMODS also measure the B-factor and structural deformity and calculate the eigenvalue. The data was examined in terms of protein and ligand root mean square deviation (RMSD), and root mean square fluctuation (RMSF).

2.7. Binding Free Energies Estimation

MMPB/GBSA methods were used to accurately predict the binding free energies (ΔG_{bind}) of the docked complex of 3' formylhonokiol and LKB1 [31]. To compute the ΔG_{bind}, a total of 200 snapshots were extracted from the last 2 ns trajectories. ΔG_{bind} was estimated as follows:

$$\Delta G_{bind} = \Delta G_{complex} - (\Delta G_{receptor} + \Delta G_{ligand})$$

2.8. ADMET Analysis

Swiss ADMET server was used to predict the effectiveness of a drug in patients. The server was assessed in order to predict the physiochemical properties, drug-likeness, pharmacokinetics of lig- and or drug, gastrointestinal absorption and brain barrier absorption [32].

3. RESULTS

3.1. Mutation Analysis

The sequence of *LKB1* gene containing 1302 bp was retrieved from NCBI using accession number U63333 (Supplementary Fig. **S1**). Using BLASTX, 23 candidate mutations were identified in LKB1 protein named as: V4A, M11V, K108R, L67P, L61V, G187S, A206E, A206V, R409G, W239R, G408A, R211S, R405K, A273T, S271N, K287R, R301Q, A318E, H379Q, Q7P, E2D, S334G, and R383S. Among the 23 identified mutations, the validation analysis through different computational tools characterized L67P and W239R for high-risk and mutational frequency in LKB1 (Supplementary Table **S1**).

3.2. Secondary Structure Prediction and Homology Modelling

Protein secondary structure was predicted using PSIPRID and polar, nonpolar, hydrophobic, aromatic plus cysteine nature of the protein was determined (Supplementary Fig. **S2**). The presence of alpha and beta-sheets was also detected. The output file showed the presence of helices as pink color, strands as orange color, and coils are grey color (Supplementary Fig. **S3**). The confidence levels of alpha helices and beta sheets were also determined and have been shown in Fig. (**1A**). From I-TASSER the 3D structure of the protein with high confidence values -1.39, TM = 0.54 ± 0.15, and RSMD score = 10.2 ± 4.6 was obtained showing 433 amino acids in the LKB1 gene (Fig. **1B**).

3.3. Molecular Docking

Three honokiol derivatives were identified and their 3D structures were downloaded from PubChem (Supplementary Table **S2**, Fig. **S4**). Before using AutoDock Vina, a target grid was prepared to detect where the ligand binds to the specific target site (Supplementary Fig. **S5A**). By using Cast p Program, activation sites on LKB1 protein were examined (Supplementary Fig. **S6**). At pocket No.1 of 3944.580 volume and 3057.526 areas, the best ligand binding site was observed, which consisted of 142 amino acids (Supplementary Fig. **S6**). The interaction analysis showed that LKB1 honokiol derivatives could bind to receptors through hydrogen bonds and non-polar interactions. The results indicated that 3'-formylhonokiol formed one hydrogen bond with LKB1 with an affinity value of -7.8, 5-formylhonokiol interacted with LKB1 through one Pi bond with an affinity value of -7.2, and 3', 5-diformylhonokiol formed one hydrogen bond with affinity value of -7.9 (Fig. **2**). The best interaction was assessed on the basis of high

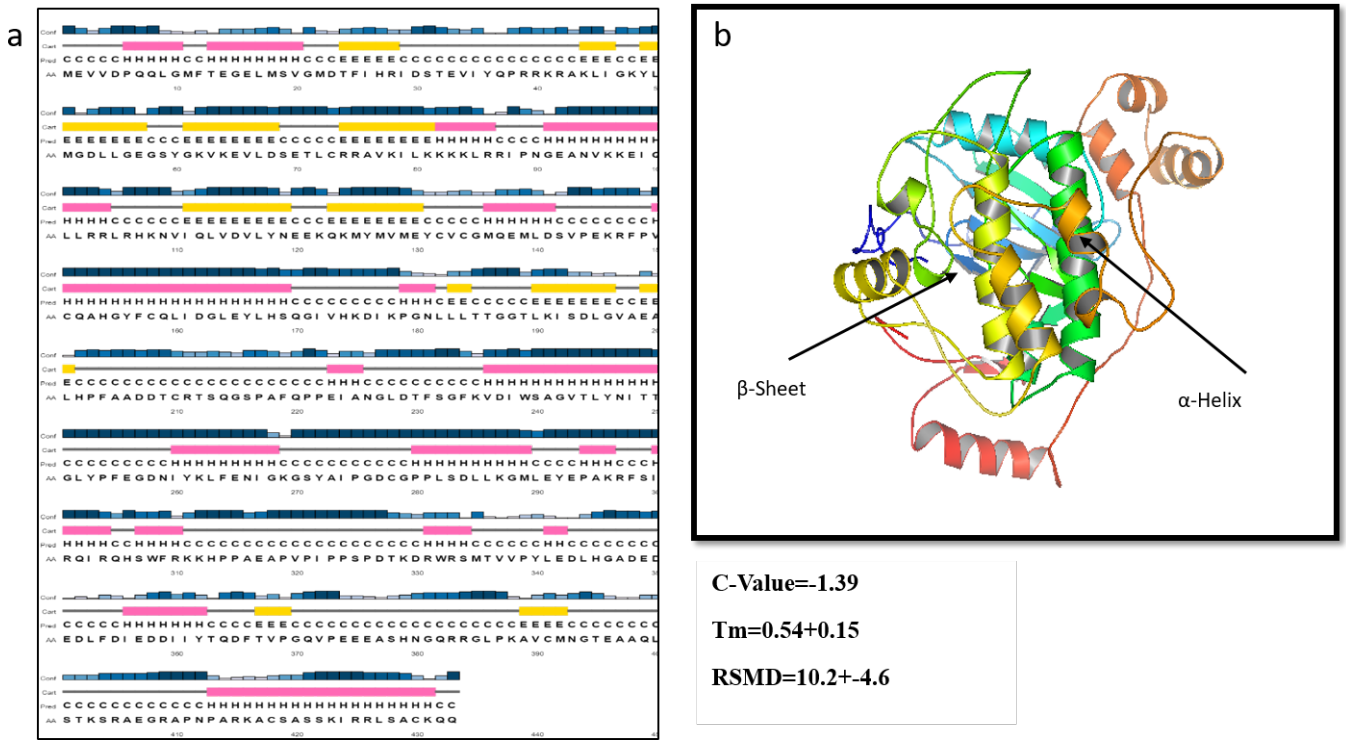

Fig. (1). Confidence prediction of α-helix, β-sheet, and coil (**A**), Protein 3-D structure (**B**). (*A higher resolution / colour version of this figure is available in the electronic copy of the article*).

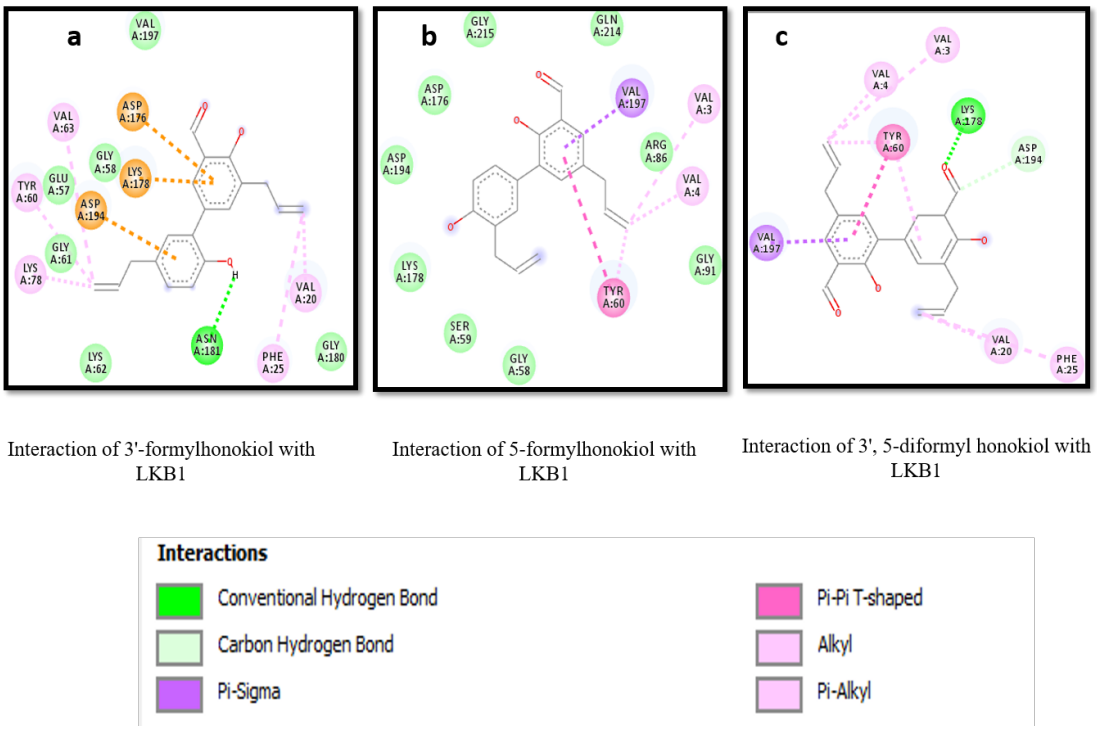

Interaction of 3'-formylhonokiol with LKB1

Interaction of 5-formylhonokiol with LKB1

Interaction of 3', 5-diformyl honokiol with LKB1

Fig. (2). The 2-dimensional views of (**a**) Interaction of 3'-formylhonokiol with LKB1, (**b**) Interaction of 5-formylhonokiol with LKB1, (**c**) Interaction of 3', 5-diformylhonokiol with LKB1 using AutoDock Vina. In each case, the hydrogen, pi-donor hydrogen, pi-alkyl, pi-sigma, and pi-anion bond interactions are shown as green, light green, purple, pink and light pink. (*A higher resolution / colour version of this figure is available in the electronic copy of the article*).

score values as the interaction between LKB1 protein and 3'-formylhonokiol had a 4836 score value as compared to LKB1 interaction with 5-formylhonokiol and 3', 5-diformylhonokiol, which showed the scores of 4824, and 4838, respectively. Through protein-ligand interaction profiler, 4 hydrophobic interactions, 2 polar hydrogen bonds, and one pi bond were observed between 3'-formylhonokiol and LKB1 protein. Hydrophobic interactions were shown as dotted lines. Subsequently, one hydrogen bond and 3 hydrophobic interactions existed between 5-formylhonokiol and the target protein. Likewise, two hydrogen bonds and five hydrophobic interactions were observed between 3', 5-diformylhonokiol and LKB1 (Supplementary Fig. **S5B** and Supplementary Fig. **S7**).

3.4. Molecular Dynamic Simulation

To optimize the selected docked complex at the atomic level and gain a better understanding of how the binding of the top-ranked ligand (3' -formylhonokiol) affects the structural and conformational stability of the protein, LKB1, 100 ns simulation was performed. As RMSD (root mean square deviation) and RMSF (root mean square fluctuations) are useful techniques for obtaining the aforementioned information for any protein/ligand docked complex, these metrics were used to investigate the resulting trajectories. Figs. (**3A** and **B**) shows the RMSDs of LKB1 complexed with 3'-formylhonokiol as well as Ligand-RMSD of 3' -formylhonokiol. The docked complex attained the equilibrium of around 10 ns while the ligand attained around 0.2 ns. The RMSD graph for the docked complex showed the initial deviations of the system with an average RMSD value of 6.02 Å, which later stabilized in the production phase with an average RMSD of 4.98 Å (Fig. **3A**). After 10 ns onwards, the RMSD value remained constant at 4.98 Å. The ligand, on the other hand, remained stable for the course of the 100 ns, with an average RMSD of 0.31 Å (Fig. **3B**). This trend in the ligand RMSD graph confirms the docking results and the stability of the ligand bound to the active site residues of the protein.

The RMSF plot showed that most of the N-terminal residues showed minimal fluctuations and less flexibility with an acceptable average value of 1.87 Å (Fig. **4**). The ligand binding site appears to have remained relatively rigid throughout the simulation. The stability and compactness of 3'-formylhonokiol with LKB1 suggested that it might be an effective activator of LKB1.

3.5. Binding Free Energies Estimation

The binding free energies of the top docked scored complex were calculated using the MMPB and MMGB methods to validate and rescore the docking results. The resulting binding free energies are calculated by subtracting the free energies of the ligand bound to the protein from the free energies of the complex's components. Negative ΔG_{bind} values for both methods indicated a strong and stable binding of 3'-formylhonokiol with *LKB*1. Table **1** shows the details of each energy component that contributed to the final values of ΔG_{bind}. Analysis of each energy component in the case of both MMGB/MMPB indicated that van der Waals interaction significantly contributed to the net ΔG_{bind}. The net value for van der Waals, for 3' formylhonokiol with two benzene rings, was -54.8280 kcal/mol^{-1}, these results were in accordance with docking results where these rings were involved in three hydrophobic interactions (Table **1**).

The collective functional motion of macromolecules was assessed through normal mode analysis (NMA) using iMODS (Internal Coordinates Normal Mode Analysis Server). IMODS performs a critical study of the structure by altering the force field of the complex with regard to the various time intervals. At each residue's capacity level, the resultant model displayed moderate deformation. The complex's region value was 7.899574e-05.cov. Heat maps with a more co-related region suggested better interaction between individual residues. Figs. (**5A-E**) depicts a full explanation of the IMODS molecular dynamic simulation. NMA mobility in the protein structure is shown in Supplementary Fig. (**S8**). The component

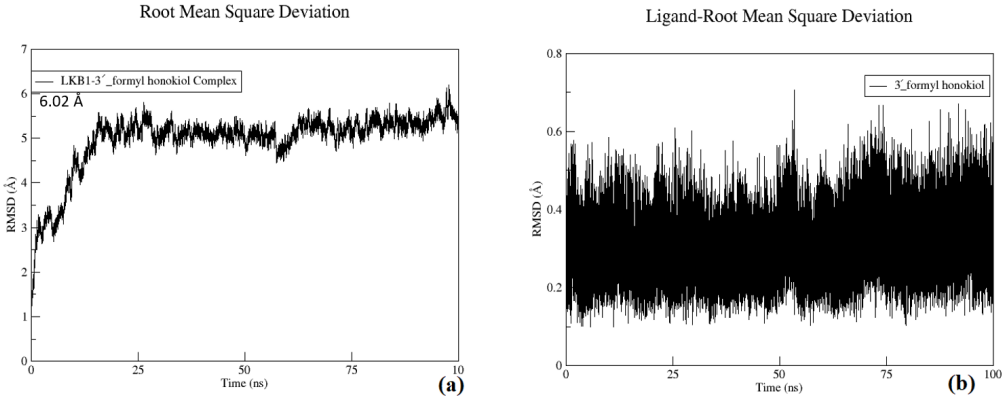

Fig. (3). The RMSD plots of drug-target complex at a variable temperatures like 300, 325, 350, 375 and 400K. (**A**) Root mean square deviation of LKB1 complexed with 3'-formylhonokiol, and (**B**) ligand-root mean square deviation of 3'-formylhonokiol. (*A higher resolution / colour version of this figure is available in the electronic copy of the article*).

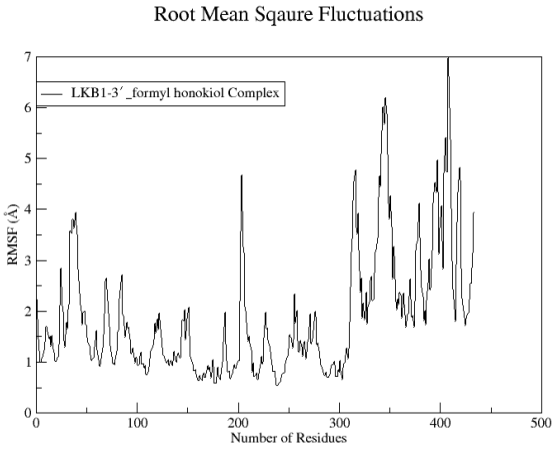

Fig. (4). The RMSF plot of LKB1-3'-formylhonokiol complex for 100 ns at 300, 325, 350, 375 and 400K. (*A higher resolution / colour version of this figure is available in the electronic copy of the article*).

Table 1. Binding free energy for the LKB1-3'-formylhonokiol complex.

MMGB		
Energy Component	**Average Value**	**Standard Deviation**
Van der Walls	-54.8280	2.5904
EEL	-10.1112	3.8683
EGB	25.4771	3.2024
ESURF	-5.8927	0.1856
ΔG_{gas}	-64.9391	4.8453
$\Delta G_{solvent}$	19.5844	3.1455
ΔG_{bind}	-45.3548	2.6875
MMPB		
Energy Component	**Average Value**	**Standard Deviation**
Van der Walls	-54.8280	2.5904
EEL	-10.1112	3.8683
EPB	40.9395	4.4803
ENPOLAR	-3.5703	0.0655
ΔG_{gas}	-64.9391	4.8453
$\Delta G_{solvent}$	37.3692	4.4907
ΔG_{bind}	-27.5699	3.8213

exhibited deformability, which revealed a moderate number of deformations at all residues as illustrated in Fig. (**5A**), whereas, the B-factor is shown in Fig. (**5B**). B-factor is based on pdb and indicated that simulation results and actual experimental pdb results were similar. A high Eigenvalue indicated the high amount of energy required to deform protein structure (Fig. **5C**), whereas high Eigenvalues are inversely related to variance indicating low levels of variance (Fig. **5D**). The red color in the covariance map indicated the interaction of the drug with the target molecule and the grey color of the elastic network represented the stiffness of the target and the difficulty in deformation (Figs. **5E** and **F**).

3.6. ADMET Analysis

The Pharmacokinetics of honokiol derivatives as boiled egg, are shown in Fig. (**S9**). The orange yolk of the egg indicates Blood Brain Barrier (BBB) and the white area represents gastrointestinal absorption. Honokiol derivatives used in this study demonstrated high gastrointestinal absorption and were blood-brain barrier permeant. As 3'-formylhonokiol and 5-formylhonokiol are isomers, they showed a similar result. Drug likeness of honokiol derivatives is shown in Table **2** and exhibited that 3'-formylhonokiol and 5-formylhonokiol followed Lipinski, Ghose, Veber, Egan and Muegge rule, whereas 3',5-diformylhonokiol violated Muegge rule. Honokiol derivatives indicated that 3'-formylhonokiol or 5-formylhonokoil, and 3',5-diformylhonokiol had lipophilicity 4.0 and 3.89 as mentioned in Tables **S3** and **S4** whereas physicochemical properties of derivatives are indicated in Table **3**.

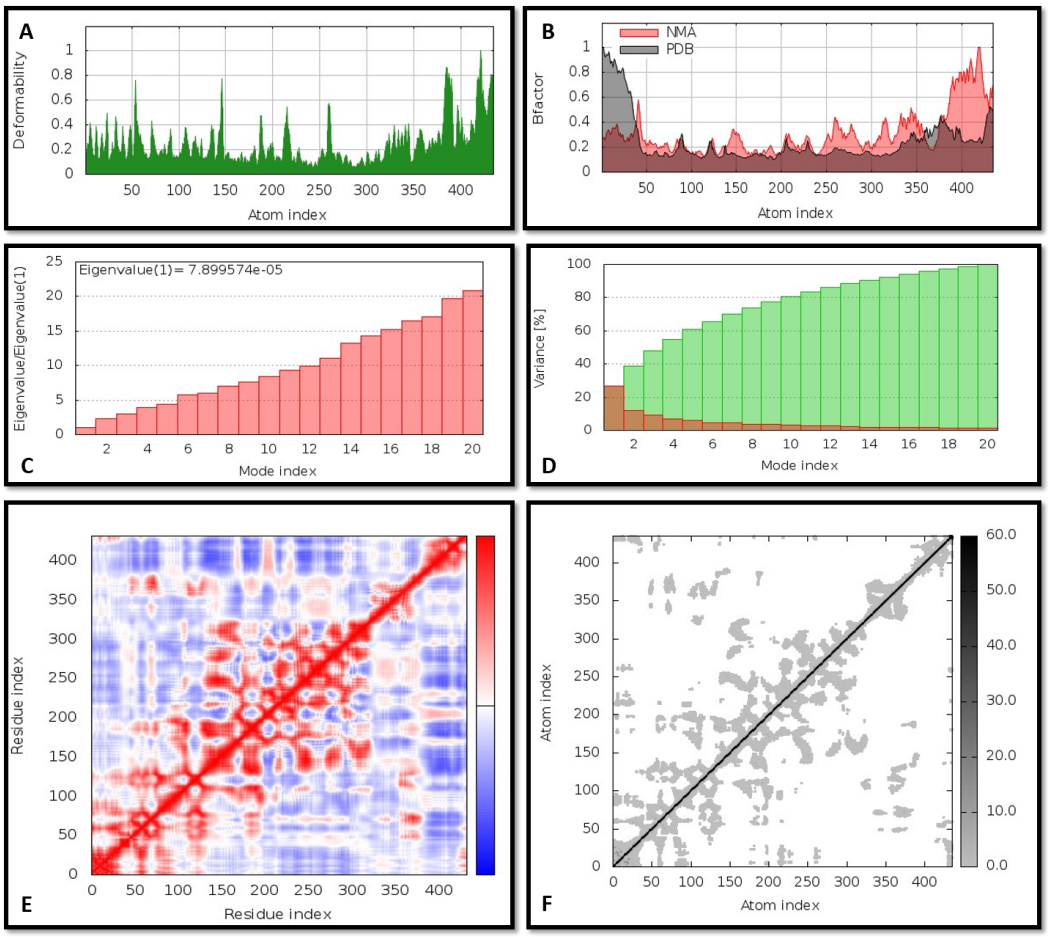

Fig. (5). Molecular dynamic simulation results showing (**A**) Deformability, (**B**) B-factor, (**C**) Eigenvalues, (**D**) Variance, (**E**) Covariance map and (**F**) Elastic network. (*A higher resolution / colour version of this figure is available in the electronic copy of the article*).

Table 2. Drug likeness of honokiol derivatives.

Rules	3'-formylhonokiol or 5-formyl honokiol	3',5-diformylhonokiol
Lipinski	Yes, 0 voilation	Yes
Ghose	Yes	Yes
Veber	Yes	Yes
Egan	Yes	Yes
Muegge	Yes	No 1 vilation XPLOG3 > 5
Bioavaiability	0.55	0.55

Table 3. Physicochemical properties of honokiol derivatives.

Physiochemical Properties	3'-formylhonokiol or 5-formyl honokiol	3', 5-diformylhonokiol
Formula	$C_{19}H_{18}O_3$	$C_{20}H_{18}O_4$
Molecular weight	294.34 g/mol	322.35
No. of heavy atoms	22	24
No. of arom. heavy atoms	12	12
Fraction csp3	0.11	0.10
No. of rotateable bond	6	7
No. of H-bond receptors	3	4
No. of H-bond donors	2	2
Molecular refrectivity	89.52	94.91

4. DISCUSSION

Honokiol is a bioactive compound of the *Magnolia officinalis* which has been extensively explored for anti-tumor and anti-apoptotic potential. Evaluation of honokiol in breast cancer cell lines was shown to inhibit both, estrogen receptor positive and negative breast cancer cell lines in a concentration and time-dependent manner. Moreover, honokiol also positively inhibited drug-resistant breast cancer cell lines through the induction of caspase-dependent apoptosis [33]. Likewise, honokiol was demonstrated for the inhibition of breast carcinogenesis through the activation of AMP-activated kinase following LKB1-dependent pathway [34]. A recent study indicated inhibition of metastasis in breast cancer cells *via* modulation of Snail/Slug protein translation. The results of the puromycin incorporation assay confirmed the honokiol-driven reduction in Snail translation efficiency and increased E-cadherin expression in metastatic nodules [35]. Another study indicating the activation of LKB1 through honokiol highlighted the multifaceted benefits of honokiol in breast cancer cell lines. The compound was shown to inhibit individual cell motility and abrogation of the stem-like phenotype of breast cancer cells through the reduction of the formation of the mammosphere [8]. More recently, studies highlighting the therapeutic potential of honokiol are experimenting with drug administration through innovative techniques. For instance, research has described the formulation and evaluation of honokiol-loaded PEGylated PLGA nanocapsules to treat breast cancer. Results of the study displayed significantly increased *in-vivo* tumor suppression in the solid Ehrlich carcinoma (SEC) breast

cancer model as compared to freely administered honokiol [36]. Likewise, honokiol was encapsulated into hyaluronic acid-modified cationic liposomes and exhibited greater cellular internalization and enhanced anti-metastatic properties [4].

Nonetheless, there are hardly any reports which describe the pharmacoinformatic approaches and virtual screening of the honokiol and its derivatives for anti-tumor potential, particularly with respect to LKB1 protein. For example, *in-silico* research studied alternate inhibitory compounds against elevated proteins in breast cancer including EGFR, HER2, and HSP90 proteins [37]. Another study focused on the synthesis and molecular docking of the 2-arylbenzothiazoles which were designed as VEGFR-2/FGFR-1/PDGFR-β multi-angiokinase inhibitors suppressing breast cancer [38]. A molecular docking analysis focusing on docking and *in-vitro* administration of adjuvant concanavalin-A displayed synergistic toxicity with co-administration of tamoxifen leading to apoptosis of estrogen-receptor positive breast cancer cells [39]. Similarly, molecular docking of quinolone derivatives provided insights into their binding affinities with topoisomerases to inhibit breast cancer [40]. Likewise, structure-based multi-targeted docking analysis of furanocoumarins was performed against breast cancer [41]. Several other molecular docking analyses studied an array of compounds for the suppression of breast cancer, nevertheless, none of them targeted honokiol and its derivatives for this purpose. This study is an effort to characterize the honokiol derivatives as potential lead drug candidates against breast cancer. Three honokiol derivatives were identified through literature based upon experimentally determined LKB1 inhibitors following the adjustment of binding energy cutoff for possible virtual hits that could act on LKB1 protein. The virtual hits were based upon LRo5 and drug-likeness, good BBB, and comprehensive ADMET profile. The best possible orientations forming stable ligand–target protein complexes, through the process of molecular docking, were achieved. Among the three derivatives, 3', 5-diformylhonokiol, and 3'-formylhonokiol, were moderately polar and showed high brain-blood barrier and gastrointestinal absorption. Besides this, the two derivatives showed the best target-binding energies and satisfied Lipinski Rules of Five, Ghose, Veber, Egan and Muggee, however, 3', 5-diformylhonokil violated Muggee rule, indicating that 3'-formylhonokiol could be used as an oral medication.

Through 100 ns simulation analysis was performed to understand the binding of the top-ranked ligand (3' -formylhonokiol) and how it affects the structural and conformational stability of the protein, LKB1. The trends in the ligand RMSD graph confirmed the docking results and the stability of the ligand bound to the active site residues of the protein. The RMSF plot showed that most of the N-terminal residues indicated minimal fluctuations and less flexibility with an acceptable average value of 1.87 Å. The ligand binding site appeared to have remained relatively rigid throughout the simulation and the stability and compactness of 3' formylhonokiol with LKB1, suggested its effective binding with LKB1. Additionally, the binding energy of the ligand and its half-life quantifies the efficiency of the ligand-protein complex and the binding energies of 3'-formylhonokiol showed strong interactions which could lead to an inhibitory reaction. This suggests the ability of the 3' -formylhonokiol to bind with mutated LKB1 protein in breast cancer cells, triggering apoptosis of cancer cells through caspase-dependent pathway or *via* endoplasmic reticulum stress-mediated apoptosis. Furthermore, all screened derivatives predicted promising ADMET profiles, and their strong binding affinity stipulated the multi-targeted potential of these selected compounds.

CONCLUSION

Molecular docking has become a powerful tool to predict drug-target interactions and discover novel therapeutics. This study was designed to explore the fundamental pharmacological properties of specific honokiol derivatives and the analysis of their binding energies at atomic levels. LKB1 protein kinase which is mutated in Peutz-Jeghers cancer syndrome, operates as a tumor suppressor. Its mutation distorts LKB1- dependent pathway which directly affects cellular polarity, low energy levels, suppression of inhibition of cell proliferation, and phosphorylation of several subsequent kinases. Honokiol and its derivatives have been reported to bind wild-type LKB1 to stimulate subsequent pathways. However, in the case of mutated LKB1 protein, honokiol, and its derivatives have not been elucidated for binding and blocking LKB1 and induction of caspase-dependent apoptosis or endoplasmic reticulum stress-mediated apoptosis. In this study, formyl derivatives of honokiol were evaluated for their enhanced solubilization for their active passage through BBB, enhancing their therapeutic window. The derivatives showed excellent PD and PK properties and can be under consideration for early drug development against breast cancer following *in-vitro* and *in-vivo* analysis.

LIST OF ABBREVIATIONS

ns	=	Nano Second
MD	=	Molecular Dynamics
GAFF	=	Generalized Amber Force Field
LKB1	=	Liver Kinase B1
AMPK	=	AMP-dependent Protein Kinase
SEC	=	Solid Ehrlich Carcinoma
BBB	=	Blood Brain Barrier
PROVEAN	=	Protein Variation Effect Analyzer
PLIP	=	Protein-ligand Interaction Profiler

ETHICS APPROVAL AND CONSENT TO PARTICIPATE

Not applicable.

HUMAN AND ANIMAL RIGHTS

Not applicable.

CONSENT FOR PUBLICATION

Not applicable.

AVAILABILITY OF DATA AND MATERIALS

All data generated or analyzed during this study are included in this published article (and its supplementary information files).

FUNDING

None.

CONFLICT OF INTEREST

The authors declare no conflict of interest, financial or otherwise.

ACKNOWLEDGEMENTS

Declared none.

SUPPLEMENTARY MATERIAL

Supplementary material is available on the publisher's website along with the published article.

REFERENCES

[1] Thun, M.J.; DeLancey, J.O.; Center, M.M.; Jemal, A.; Ward, E.M. The global burden of cancer: Priorities for prevention. *Carcinogenesis,* **2010**, *31*(1), 100-110.

http://dx.doi.org/10.1093/carcin/bgp263 PMID: 19934210

[2] Chaudhari, S.K.; Arshad, S.; Amjad, M.S.; Akhtar, M.S. Natural compounds extracted from medicinal plants and their applications. In: *Natural Bio-active Compounds*; Springer: Singapore, **2019**; pp. 193-207.
http://dx.doi.org/10.1007/978-981-13-7154-7_7

[3] Bai, X.; Cerimele, F.; Ushio-Fukai, M.; Waqas, M.; Campbell, P.M.; Govindarajan, B.; Der, C.J.; Battle, T.; Frank, D.A.; Ye, K.; Murad, E.; Dubiel, W.; Soff, G.; Arbiser, J.L. Honokiol, a small molecular weight natural product, inhibits angiogenesis *in vitro* and tumor growth *in vivo*. *J. Biol. Chem.,* **2003**, *278*(37), 35501-35507.
http://dx.doi.org/10.1074/jbc.M302967200 PMID: 12816951

[4] Wang, J.; Liu, D.; Guan, S.; Zhu, W.; Fan, L.; Zhang, Q.; Cai, D. Hyaluronic acid-modified liposomal honokiol nanocarrier: Enhance anti-metastasis and antitumor efficacy against breast cancer. *Carbohydr. Polym.,* **2020**, *235*, 115981.
http://dx.doi.org/10.1016/j.carbpol.2020.115981 PMID: 32122511

[5] Katiyar, S. Emerging phytochemicals for the prevention and treatment of head and neck cancer. *Molecules,* **2016**, *21*(12), 1610.
http://dx.doi.org/10.3390/molecules21121610 PMID: 27886147

[6] Pan, J.; Lee, Y.; Wang, Y.; You, M. Honokiol targets mitochondria to halt cancer progression and metastasis. *Mol. Nutr. Food Res.,* **2016**, *60*(6), 1383-1395.
http://dx.doi.org/10.1002/mnfr.201501007 PMID: 27276215

[7] Vaahtomeri, K.; Mäkelä, T.P. Molecular mechanisms of tumor suppression by LKB1. *FEBS Lett.,* **2011**, *585*(7), 944-951.
http://dx.doi.org/10.1016/j.febslet.2010.12.034 PMID: 21192934

[8] Sengupta, S.; Nagalingam, A.; Muniraj, N.; Bonner, M.Y.; Mistriotis, P.; Afthinos, A.; Kuppusamy, P.; Lanoue, D.; Cho, S.; Korangath, P.; Shriver, M.; Begum, A.; Merino, V.F.; Huang, C-Y.; Arbiser, J.L.; Matsui, W.; Győrffy, B.; Konstantopoulos, K.; Sukumar, S.; Marignani, P.A.; Saxena, N.K.; Sharma, D. Activation of tumor suppressor LKB1 by honokiol abrogates cancer stem-like phenotype in breast cancer *via* inhibition of oncogenic Stat3. *Oncogene,* **2017**, *36*(41), 5709-5721.
http://dx.doi.org/10.1038/onc.2017.164 PMID: 28581518

[9] Fried, L.E.; Arbiser, J.L. Honokiol, a multifunctional antiangiogenic and antitumor agent. *Antioxid. Redox Signal.,* **2009**, *11*(5), 1139-1148.
http://dx.doi.org/10.1089/ars.2009.2440 PMID: 19203212

[10] Adzhubei, I.A.; Schmidt, S.; Peshkin, L.; Ramensky, V.E.; Gerasimova, A.; Bork, P.; Kondrashov, A.S.; Sunyaev, S.R. A method and server for predicting damaging missense mutations. *Nat. Methods,* **2010**, *7*(4), 248-249.
http://dx.doi.org/10.1038/nmeth0410-248 PMID: 20354512

[11] Vaser, R.; Adusumalli, S.; Leng, S.N.; Sikic, M.; Ng, P.C. SIFT missense predictions for genomes. *Nat. Protoc.,* **2016**, *11*(1), 1-9.
http://dx.doi.org/10.1038/nprot.2015.123 PMID: 26633127

[12] Capriotti, E.; Fariselli, P. PhD-SNP^g: A webserver and lightweight tool for scoring single nucleotide variants. *Nucleic Acids Res.,* **2017**, *45*(W1), W247-W252.
http://dx.doi.org/10.1093/nar/gkx369 PMID: 28482034

[13] Pejaver, V.; Urresti, J.; Lugo-Martinez, J.; Pagel, K.A.; Lin, G.N.; Nam, H.J.; Mort, M.; Cooper, D.N.; Sebat, J.; Iakoucheva, L.M.; Mooney, S.D.; Radivojac, P. Inferring the molecular and phenotypic impact of amino acid variants with MutPred2. *Nat. Commun.,* **2020**, *11*(1), 5918.
http://dx.doi.org/10.1038/s41467-020-19669-x PMID: 33219223

[14] Capriotti, E.; Fariselli, P.; Casadio, R. I-Mutant2.0: Predicting stability changes upon mutation from the protein sequence or structure. *Nucleic Acids Res.,* **2005**, *33*, W306-W310.
http://dx.doi.org/10.1093/nar/gki375 PMID: 15980478

[15] Choi, Y.; Chan, A.P.; Qin, B.; Zhang, Y.; Liu, X.S. PROVEAN web server: A tool to predict the functional effect of amino acid substitutions and indels. *Bioinformatics,* **2015**, *31*(16), 2745-2747.
http://dx.doi.org/10.1093/bioinformatics/btv195 PMID: 25851949

[16] Buchan, D.W.A.; Minneci, F.; Nugent, T.C.O.; Bryson, K.; Jones, D.T. Scalable web services for the PSIPRED protein analysis workbench. *Nucleic Acids Res.,* **2013**, *41*(W1), W349-W357.
http://dx.doi.org/10.1093/nar/gkt381 PMID: 23748958

[17] Zhang, Y. I-TASSER server for protein 3D structure prediction. *BMC Bioinformatics,* **2008**, *9*(1), 40.
http://dx.doi.org/10.1186/1471-2105-9-40 PMID: 18215316

[18] Kim, S.; Chen, J.; Cheng, T.; Gindulyte, A.; He, J.; He, S.; Li, Q.; Shoemaker, B.A.; Thiessen, P.A.; Yu, B.; Zaslavsky, L.; Zhang, J.; Bolton, E.E. PubChem in 2021: New data content and improved web interfaces. *Nucleic Acids Res.,* **2021**, *49*(D1), D1388-D1395.
http://dx.doi.org/10.1093/nar/gkaa971 PMID: 33151290

[19] Kolpakov, F.A.; Babenko, V.N. Computer system MGL: Tool for sample generation, visualization, and analysis of regulatory genomic sequences. *Mol. Biol.,* **1997**, *31*, 540-547.

[20] Tian, W.; Chen, C.; Lei, X.; Zhao, J.; Liang, J.; Jiang, S.; Zhou, Y.; Du, L. CASTp 3.0: computed atlas of surface topography of proteins. *Nucleic Acids Res.,* **2018**, *46*(W1), W363-W367.
http://dx.doi.org/10.1093/nar/gky473 PMID: 29860391

[21] Yuan, S.; Chan, H.C.S.; Hu, Z. Using PYMOL as a platform for computational drug design. *Wiley Interdiscip. Rev. Comput. Mol. Sci.,* **2017**, *7*(2), e1298.
http://dx.doi.org/10.1002/wcms.1298

[22] Schneidman-Duhovny, D.; Inbar, Y.; Nussinov, R.; Wolfson, H.J. PatchDock and SymmDock: Servers for rigid and symmetric docking. *Nucleic Acids Res.,* **2005**, *33*, W363-W367.
http://dx.doi.org/10.1093/nar/gki481 PMID: 15980490

[23] Adasme, M.F.; Linnemann, K.L.; Bolz, S.N.; Kaiser, F.; Salentin, S.; Haupt, V.J.; Schroeder, M.; Damore, M.A.; Boedigheimer, M.; Blomme, E.; Ciurlionis, R. PLIP 2021: Expanding the scope of the protein-ligand interaction profiler to DNA and RNA. *Nucleic Acids Res.,* **2021**, *49*(W1), W530-W534.
http://dx.doi.org/10.1093/nar/gkab294 PMID: 33950214

[24] Case, D.A.; Darden, T.A.; Cheatham, T.E.; Simmerling, C.L.; Wang, J.; Duke, R.E.; Luo, R.; Crowley, M.R.; Walker, R.C.; Zhang, W.; Merz, K.M. AMBER 10; University of California; San Francisco, **2008**.

[25] Frisch, M.J.; Trucks, G.W.; Schlegel, H.B.; Scuseria, G.E.; Robb, M.A.; Cheeseman, J.R.; Scalmani, G.; Barone, V. Gaussian 09, Revision A.02*;* Gaussian, Inc.: Wallingford, CT, **2016**.

[26] Eggimann, B.L.; Sunnarborg, A.J.; Stern, H.D.; Bliss, A.P.; Siepmann, J.I. An online parameter and property database for the TraPPE force field. *Mol. Simul.,* **2014**, *40*(1-3), 101-105.
http://dx.doi.org/10.1080/08927022.2013.842994

[27] Hornak, V.; Abel, R.; Okur, A.; Strockbine, B.; Roitberg, A.; Simmerling, C. Comparison of multiple Amber force fields and development of improved protein backbone parameters. *Proteins,* **2006**, *65*(3), 712-725.
http://dx.doi.org/10.1002/prot.21123 PMID: 16981200

[28] Case, D.A.; Cheatham, T.E., III; Darden, T.; Gohlke, H.; Luo, R., Jr; Merz, K.M., Jr; Onufriev, A.; Simmerling, C.; Wang, B.; Woods, R.J. The Amber biomolecular simulation programs. *J. Comput. Chem.,* **2005**, *26*(16), 1668-1688.
http://dx.doi.org/10.1002/jcc.20290 PMID: 16200636

[29] Jorgensen, W.L.; Chandrasekhar, J.; Madura, J.D.; Impey, R.W.; Klein, M.L. Comparison of simple potential functions for simulating liquid water. *J. Chem. Phys.,* **1983**, *79*(2), 926-935.
http://dx.doi.org/10.1063/1.445869

[30] Darden, T.; York, D.; Pedersen, L. Particle mesh Ewald: An $N \cdot \log(N)$ method for Ewald sums in large systems. *J. Chem. Phys.,* **1993**, *98*(12), 10089-10092.
http://dx.doi.org/10.1063/1.464397

[31] Miller, B.R., III; McGee, T.D., Jr; Swails, J.M.; Homeyer, N.; Gohlke, H.; Roitberg, A.E. MMPBSA.py: An efficient program for end-state free energy calculations. *J. Chem. Theory Comput.,* **2012**, *8*(9), 3314-3321.
http://dx.doi.org/10.1021/ct300418h PMID: 26605738

[32] Mermelstein, D.J.; Lin, C.; Nelson, G.; Kretsch, R.; McCammon, J.A.; Walker, R.C. Fast and flexible gpu accelerated binding free energy calculations within the amber molecular dynamics package. *J. Comput. Chem.,* **2018**, *39*(19), 1354-1358.
http://dx.doi.org/10.1002/jcc.25187 PMID: 29532496

[33] Liu, H.; Zang, C.; Emde, A.; Planas-Silva, M.D.; Rosche, M.; Kühnl, A.; Schulz, C.O.; Elstner, E.; Possinger, K.; Eucker, J. Anti-tumor effect of honokiol alone and in combination with other anti-cancer agents in breast cancer. *Eur. J. Pharmacol.,* **2008**, *591*(1-3), 43-51.
http://dx.doi.org/10.1016/j.ejphar.2008.06.026 PMID: 18588872

[34] Nagalingam, A.; Arbiser, J.L.; Bonner, M.Y.; Saxena, N.K.; Sharma, D. Honokiol activates AMP-activated protein kinase in breast cancer cells *via* an LKB1-dependent pathway and inhibits breast carcinogenesis. *Breast Cancer Res.,* **2012**, *14*(1), R35.
http://dx.doi.org/10.1186/bcr3128 PMID: 22353783

[35] Wang, W.; Shang, Y.; Li, Y.; Chen, S. Honokiol inhibits breast cancer cell metastasis by blocking EMT through modulation of

Snail/Slug protein translation. *Acta Pharmacol. Sin.,* **2019**, *40*(9), 1219-1227.
http://dx.doi.org/10.1038/s41401-019-0240-x PMID: 31235819

[36] Haggag, Y.A.; Ibrahim, R.R.; Hafiz, A.A. Design, formulation and *in vivo* evaluation of novel honokiol-loaded PEGylated PLGA nanocapsules for treatment of breast cancer. *Int. J. Nanomedic.,* **2020**, *15*, 1625-1642.
http://dx.doi.org/10.2147/IJN.S241428 PMID: 32210557

[37] Yousuf, Z.; Iman, K.; Iftikhar, N.; Mirza, M. Structure-based virtual screening and molecular docking for the identification of potential multi-targeted inhibitors against breast cancer. *Breast Cancer,* **2017**, *9*, 447-459.
http://dx.doi.org/10.2147/BCTT.S132074 PMID: 28652811

[38] Abdel-Mohsen, H.T.; Abd El-Meguid, E.A.; El Kerdawy, A.M.; Mahmoud, A.E.E.; Ali, M.M. Design, synthesis, and molecular docking of novel 2-arylbenzothiazole multiangiokinase inhibitors targeting breast cancer. *Arch. Pharm.,* **2020**, *353*(4), 1900340.
http://dx.doi.org/10.1002/ardp.201900340 PMID: 32045054

[39] Elshal, M.; Eid, N.; El-Sayed, I.; El-Sayed, W.; Al-Karmalawy, A.A. Concanavalin-A shows synergistic cytotoxicity with tamoxifen *via* inducing apoptosis in estrogen receptor-positive breast cancer: *In vitro* and molecular docking studies. *Ulum-i Daruyi,* **2021**, *28*, 76-85.
http://dx.doi.org/10.34172/PS.2021.22

[40] Idris, M.O.; Adeniji, S.E.; Habib, K.; Adeiza, A.A. Molecular docking of some novel quinoline derivatives as potent inhibitors of human breast cancer cell line. *Lab-in-Silico,* **2021**, *2*, 30-37.
http://dx.doi.org/10.22034/labinsilico21021030

[41] Acharya, R.; Chacko, S.; Bose, P.; Lapenna, A.; Pattanayak, S.P. Structure based multitargeted molecular docking analysis of selected furanocoumarins against breast cancer. *Sci. Rep.,* **2019**, *9*(1), 15743.
http://dx.doi.org/10.1038/s41598-019-52162-0 PMID: 31673107